

Lithium-based surfaces controlling fusion plasma behavior at the plasma-material interface^{a)}

Jean Paul Allain^{b)} and Chase N. Taylor

School of Nuclear Engineering, Purdue University, 400 Central Avenue, West Lafayette, Indiana 47907, USA

(Received 2 December 2011; accepted 26 April 2012; published online 31 May 2012)

The plasma-material interface and its impact on the performance of magnetically confined thermonuclear fusion plasmas are considered to be one of the key scientific gaps in the realization of nuclear fusion power. At this interface, high particle and heat flux from the fusion plasma can limit the material's lifetime and reliability and therefore hinder operation of the fusion device. Lithium-based surfaces are now being used in major magnetic confinement fusion devices and have observed profound effects on plasma performance including enhanced confinement, suppression and control of edge localized modes (ELM), lower hydrogen recycling and impurity suppression. The critical spatial scale length of deuterium and helium particle interactions in lithium ranges between 5–100 nm depending on the incident particle energies at the edge and magnetic configuration. Lithium-based surfaces also range from liquid state to solid lithium coatings on a variety of substrates (e.g., graphite, stainless steel, refractory metal W/Mo/etc., or porous metal structures). Temperature-dependent effects from lithium-based surfaces as plasma facing components (PFC) include magnetohydrodynamic (MHD) instability issues related to liquid lithium, surface impurity, and deuterium retention issues, and anomalous physical sputtering increase at temperatures above lithium's melting point. The paper discusses the viability of lithium-based surfaces in future burning-plasma environments such as those found in ITER and DEMO-like fusion reactor devices. © 2012 American Institute of Physics. [<http://dx.doi.org/10.1063/1.4719688>]

I. INTRODUCTION

Lithium has reached an important feat in the context of plasma-facing materials in thermonuclear magnetic fusion devices. Lithium-based surfaces are now routinely used in numerous magnetically confined fusion devices around the world.^{1–6} The study of lithium as a plasma-facing surface (PFS) had its beginnings with the work of Erents and McCracken in the early 1970s.⁷ However, the first result demonstrating direct correlation between lithium-based surfaces and the behavior of the core fusion plasma was Mansfield's application of lithium coatings on the hot graphite limiter in the Tokamak Fusion Test Reactor (TFTR).⁸ This result culminated in some of the best confinement shots for TFTR. The hypothesis at the time was the unique high affinity of lithium for hydrogen. Shortly after this result in an effort to elucidate on the groundbreaking results with lithium in TFTR, H. Sugai and his group embarked on a series of off-line laboratory experiments to study the properties of lithium coatings on graphite.^{9,10} Lithium is well known in the lithium battery community and dominant intercalation mechanisms were identified by Itou and Sugai's work in a number of landmark experiments.¹¹ However, these results opened up a more serious mystery. How were ultra-thin films of lithium on graphite capable of affecting the core plasma behavior in TFTR, in particular, since lithium readily intercalates into graphite? The answer to this question implied

that the chemical condition of the surface played a critical role on this control as also mentioned by Mansfield and Sugai in their respective papers.

In parallel to this work efforts in the United States, after its temporary exit from the international thermonuclear experimental reactor (ITER) project in the mid-1990s, began to focus on advanced concepts for divertor and limiter materials as well as innovative fusion chamber technology concepts with the ALPS (Advanced Limiter-divertor Plasma-facing Systems) and APEX (Advanced Power EXtraction) programs, respectively.^{12–14} In particular, the ALPS program became an effort to study the viability of liquid-based surfaces as plasma-facing materials. Lithium became one of the leading alternative plasma facing component (PFC) materials due to its attractive heat extraction properties as well as potential low-recycling hydrogen characteristics.

Lithium-based surfaces were therefore studied in a variety of settings. T-11M successfully operated 2×10^3 plasma shots using a lithium capillary pore system (CPS).² The primary experimental objective was to demonstrate that by taking advantage of liquid capillary forces, liquid lithium could be introduced without splashing and inducing major disruptions in plasma operations. FTU (Frascati Tokamak Upgrade) operated with a liquid lithium limiter since 2005 and found 20% enhancement in energy confinement time.⁴ Doerner and Baldwin conducted the first studies on hydrogen retention and lithium sputtering using a linear plasma device,^{15–18} shortly after, Bastasz and Whaley conducted surface analysis of lithium-based surfaces with low-energy ion scattering spectroscopy (LEISS).¹⁹ In parallel, Allain and

^{a)}Paper P12 6, Bull. Am. Phys. Soc. 56, 228 (2011).

^{b)}Invited speaker. Electronic mail: allain@purdue.edu.

Ruzic studied the fundamental physical sputtering mechanisms of lithium-based surfaces in a well-controlled particle-beam experiment.²⁰

Continuing the use of lithium-based PFC work, Majeski and Kaita pioneered the use of a liquid lithium divertor torus sector that resulted in some of the most convincing evidence of lithium's low recycling capability, in addition to showing improvements in nearly every measurable plasma physics parameter.^{21,22} Lithium coatings on the National Spherical Torus Experiment (NSTX) by Kugel *et al.* then followed with exciting results, including the suppression of edge disruptions.^{23,24} In this case, NSTX began lithium depositions using pellet injection, then progressed to using one and then two evaporators to deposit lithium on ATJ graphite tiles. Since 2004, Allain *et al.* has been investigating details of surface chemistry and surface physics of lithiated graphite.

The most important pressing questions that came from nearly a decade of work on lithium-based surfaces were primarily: what is the key mechanism(s) for D and He retention in lithium both in the solid and liquid states? What is the temperature window range for a viable lithium-based PFI (plasma-facing interface) under burning plasma conditions? What is the surface chemistry of liquid lithium surfaces? What about lithium coatings on graphite? How are impurities controlled by lithium on metallic or graphitic substrates?

This paper focuses on presenting the most salient results on lithium-based surfaces and their chemical and physical properties in the context of their use as a plasma-material interface. The paper also outlines outstanding issues to date and also discusses the viability of lithium-based surfaces in future burning-plasma environments such as those found in ITER and DEMO-like fusion reactor devices.

II. EXPERIMENTAL RESULTS

A. Liquid lithium

Studies of liquid lithium-based surfaces in the late 1990s focused on establishing the physical basis for their use as a plasma-facing material.²⁵ Three primary laboratory experiment efforts were conducted, which focused strictly on plasma and particle-beam surface interactions. First the use of a high-intensity linear plasma device, PISCES-B (Plasma Interaction with Surface and Components Experimental Simulator-B), that exposed solid and liquid lithium samples to a variety of linear plasma conditions.²⁶ Second, the work by Bastasz and Whaley focused on low-energy ion scattering spectroscopy and direct recoil spectroscopy studies to elucidate on the surface physics of the liquid lithium surface.^{19,27} Lastly, the work by Allain and Ruzic focused on the study of physical sputtering from controlled particle-beam interactions under a variety of surface conditions from lithium-based surfaces.^{20,28}

Doerner and Baldwin discovered in early 2000 the anomalous increase in lithium sputtering as the temperature of the sample was increased.¹⁸ This result was considered abnormal given that the temperature levels of the sample only rose to about twice the melting point of lithium (e.g., 180 °C) and thus evaporative mechanisms were not dominant. Whyte and Doerner also measured the sputtered energy distribution using

optical emission spectroscopy (OES) measurements and found that the average energy of the emitted particles varied between 1 and 0.3 eV as the temperature rose from melting 200 °C up to about 400 °C.²⁶ Shortly after Allain and Ruzic confirmed this anomalous increase with numerous controlled particle-beam experiments.²⁰ The ion-beam facility allowed for *in-situ* measurement of erosion during the independent increase in temperature of the liquid Li sample. At each temperature, the component due to evaporation was accounted for and the result led to a similar anomalous increase in the physical sputter yield of lithium.

Fig. 1 shows a comparison of various D-treated temperature-dependent lithium erosion ion-beam based experiments using the IIAX (ion-surface interaction experiment) device by Allain *et al.*²⁰ These results corroborated plasma-based lithium erosion experiments by Doerner *et al.* where the lithium sputter yield increased non-linearly with temperature. The primary difference between these two experiments was the sequence of exposures and flux magnitude of incident deuterium particles. In the PISCES-B experiments, a solid lithium foil sample was exposed to high-intensity deuterium plasmas. The sample was biased to a pre-determined voltage that dictates the energy of the incident particles. The bias can be varied to control the incident particle energy. The emission of atoms from the surface was then measured via optical emission spectroscopy using a Li I line filter. Knowing the SX/B ratio one can obtain absolute values of the sputter yield *in-situ* during irradiation. The plasma also heats the sample and emission of particles can be obtained using OES during increase of the surface temperature. The ion-beam laboratory experiments are different. The incident ion energy can be controlled independent of the surface temperature. The sputtered particles are also collected with a quartz crystal microbalance calibrated at each sample temperature. Evaporation is subtracted at each sample temperature and thus only the physical sputtering component is measured. Results showed the non-linear rate of increase of the sputter yield with temperature to be much higher for the linear plasma results compared to the particle-beam results in IIAX, thus owing to a flux-dependent mechanism in addition to the thermal mechanism discovered in both experiments.

The results of Fig. 1 show ion-beam data from IIAX compared to the VFTRIM-3D sputtering models developed by Allain and Ruzic.^{29,30} The anomalous increase in sputter yield was in fact also observed in tokamak plasma material interaction (PMI) experiments including Li DiMES (Ref. 31) and by Mirnov *et al.* in T11.³² Both cases consisted of an incident ion flux orders of magnitude higher than the particle-beam results in IIAX. This enhancement had a unique correlation between near-surface energy deposition mechanisms and erosion. Namely, near-surface thermal spikes were conjectured to be partly responsible for the enhanced increase of sputtering with temperature. In Fig. 2, the temperature-dependent data is plotted against a factor for the energy deposition distribution in lithium. Conventional increase of the sputter yield with energy scales as $X^{1/2}$ and when "thermal spike" effects are invoked a stronger increase is found scaling as $X^{7/3}$. Several models by Allain *et al.* have explored this relationship using TRIM-SP (transport of ions in matter-sputtering) Monte Carlo simulation codes with

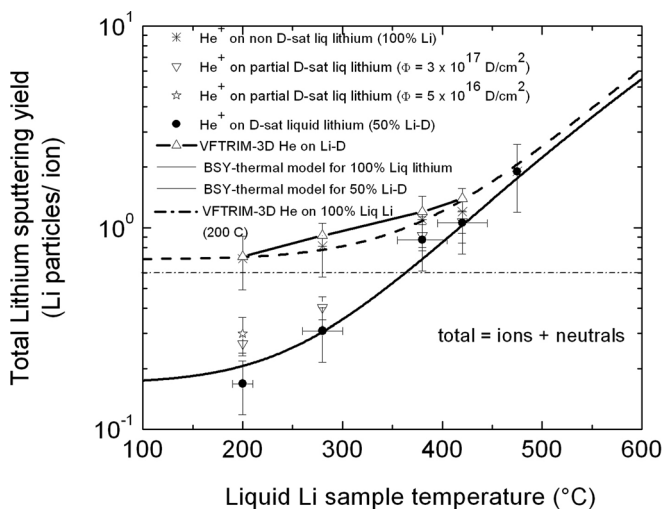


FIG. 1. The lithium sputter yield of lithium atoms as a function of system temperature for He+ irradiation at 45° incidence. Comparison of temperature-dependent sputtering for various D coverages on lithium surfaces.

modified recoil spectra to arbitrarily vary the energy deposition density fields near the surface tuned to the measured temperature-dependent yields.³⁰ The best fits to the experimental yields are found only when the modified energy distribution spectra (found with molecular dynamics simulations, see Ref. 30) and temperature-dependent surface binding energy, U (U calibrated to measured emitted energy spectra in PISCES and IIAX), are shifted to lower sputtered energies. This particular phenomenon was identified in measured current-voltage (I-V) traces conducted on liquid lithium samples. The I-V measurements consisted of high resolution biasing of the lithium-based sample that ultimately resulted in the first measurement of the secondary ion sputtered fraction by Allain.³³

Fig. 3 shows the I-V traces taken for He ion bombardment at 700 eV on liquid lithium at various sample temperatures. These traces represent the amount of current collected with a detector juxtaposed to the sputtered plume of the lithium-based target. The target is biased in order to suppress the sputtered ion current. Thus a simple fraction of sputtered

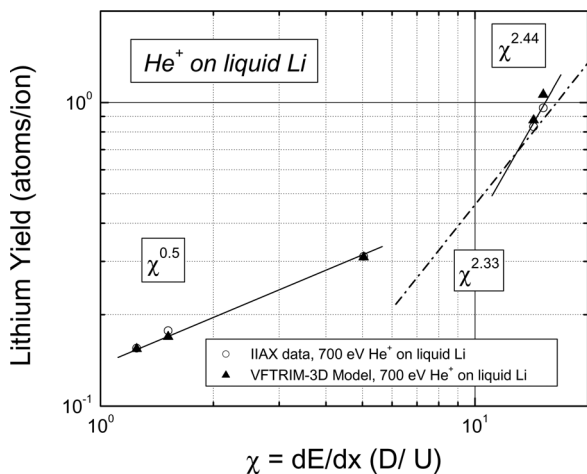


FIG. 2. Non-linear erosion regime of lithium sputter yield under He+ irradiation on liquid lithium. Lithium sputter yield plotted against the energy deposition.

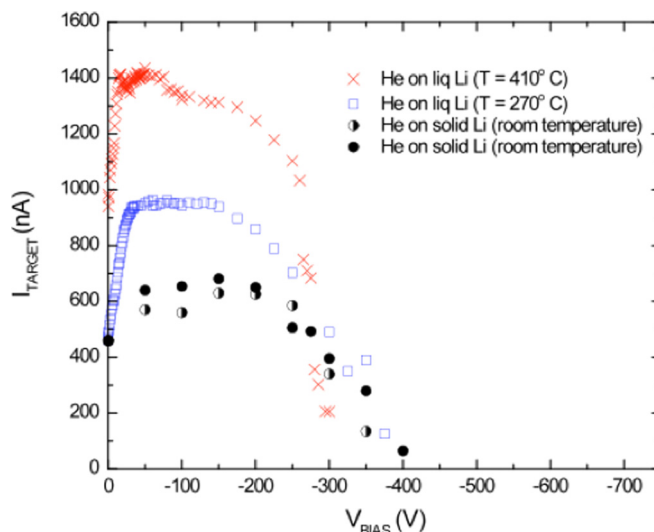


FIG. 3. I-V traces indicating secondary ion sputtered ion distributions for He irradiation at 700 eV on solid and liquid Li.

ions to atoms is obtained as a function of voltage (i.e., corresponding to the particle energy). The sputtered ion distributions were extracted from the I-V data and correlated with the non-linear temperature enhancement observed in the sputter yields. Note that for temperatures between 270 °C and 410 °C, the channel for sputtered ions at lower energy rises in addition to the conventional sputtered distributions as shown for room temperature data and dictated by the known Thompson distribution. This behavior is indicative of thermal-like sputtering behavior observed by Thompson in his laboratory.³⁴

B. Lithium-based alloys

Lithium-based alloys such as FLiBe (a molten salt comprised of fluorine, lithium, and beryllium) and SnLi were considered as possible alternate materials to pure liquid lithium.^{27,28,35} The key limitation with FLiBe as a plasma-facing surface was, namely, the nature of chemical sputtering from these systems. Chemical erosion stemmed from volatile F-based molecules and complexes emitted by their interaction with lithium and beryllium, in part due to strong oxygen gettering properties. FLiBe, however, did not receive enough attention with systematic experiments to understand its viability as a PFC material and therefore more work is needed in this regard. Sputtering of levels near 0.1 to 0.7 F atoms/ion for energies between 100 and 1000 eV were found with TRIM-SP simulations.³⁶

Extensive surface science studies by Bastasz and Allain on the SnLi system have been completed in the context of surface composition and physical sputtering, respectively.^{19,28} Surface composition of SnLi is dominated by a thin segregated layer of lithium atoms when the sample reaches its melting point around 320 °C for the 20% Li-Sn eutectic concentration. Bastasz measured the surface concentration as a function of temperature and at 320 °C lithium dominates the concentration. Allain *et al.* observed this segregation mechanism indirectly in two ways.³³ First the sputter yield from eutectic 0.8 Sn-Li alloy as a function of temperature and energy was conducted at energies

200–1000 eV with D^+ and He^+ irradiation. Characterization of the collected sputtered material with SIMS (secondary ion mass spectrometry) measured composition of collected sputtered particles was dominated by lithium atoms (>90%). Fig. 4 shows results for the temperature-dependent lithium sputter yield of 80%-Sn-Li surface by low-energy D and He irradiation. Also, note that the threshold for temperature-dependent enhancement of sputtering is increased to higher system temperatures near 350 °C. This is clearly an indication that the enhancement was linked to a thermal-activated mechanism.

The observed threshold for the enhanced sputter yield from 0.8 Sn-Li alloy surfaces is not unusual since the theoretical evaporative thermal-activated flux is about 10^5 times less for the 0.8 Sn-Li alloy compared to pure lithium at 300 °C as shown in Fig. 5. Notably the segregated lithium layer on liquid 0.8 Sn-Li surfaces had similar behavior to pure liquid Li surfaces, in particular the 2/3 fraction of sputtered particles as ions. Furthermore, the enhancement threshold also shows dependence with incident species mass (e.g., 350 °C for He and ~ 400 °C for D irradiation) indicating that not only is the enhancement a thermal-activated mechanism but also a collisional mechanism near the liquid-metal surface. This finding is critical, given the narrow temperature window for liquid lithium as a potential PFC candidate material. The promise of having a “lithium-like” surface yet with a relatively wider temperature window is an attractive prospect that needs further investigation, in particular under conditions of future reactor fusion device conditions. The “lithium-dominated” surface is also attractive from the standpoint of radiative losses inherent with high-Z materials. For example, the relative fractional impurity level that leads to an equivalent radiative loss of 50% the alpha heating power from emitted Li atoms into the core plasma is a factor of 10^3 higher than for tin atoms! In fact, the fractional impurity level for Sn atoms emitted into the plasma is about 0.03% compared to 0.07% for molybdenum. This means that even a small Sn flux into the plasma could easily quench it. Therefore, replenishment of the surface with lithium atoms in the Sn-Li alloy is essential to manage radiative losses

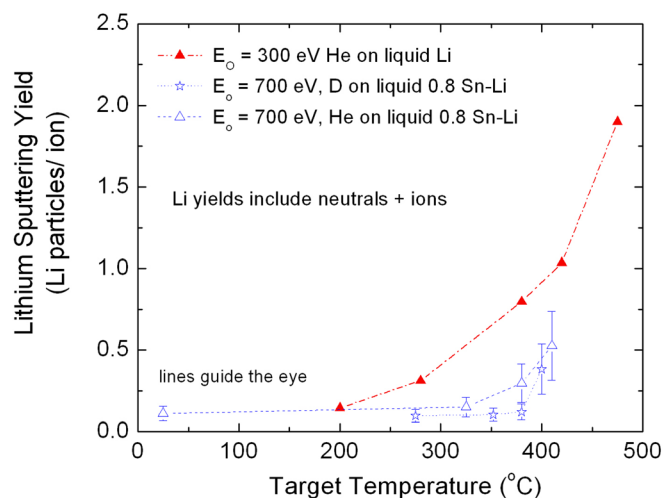


FIG. 4. Sputtering yield of Li atoms per D or He irradiation at 700 eV as a function of sample temperature and with correction for evaporation.

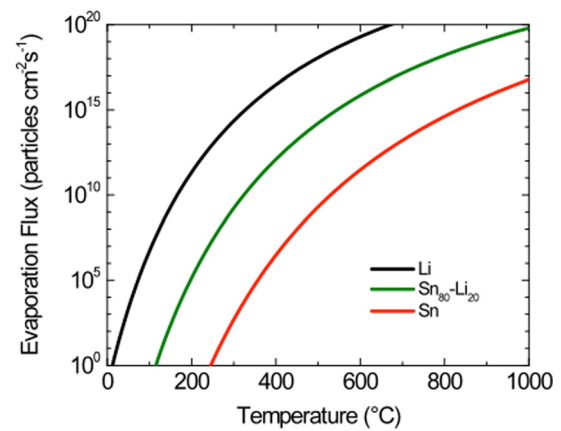


FIG. 5. Evaporation flux of lithium as a function of system temperature from Li, 0.8 Sn-Li eutectic alloy and tin.

from PMI using this plasma-facing surface. Bastasz and Eckstein estimated that for temperatures above 450 °C one could maintain a mostly liquid Li surface layer (e.g., about 60%–70% of Li on surface) due to temperature-dominated Gibbsian surface segregation of lithium atoms to the Sn-Li alloy surface.³⁵

In addition to the temperature-dependent findings illustrated by the work on liquid Sn-Li, another important study examined D retention after irradiation and compared to pure liquid lithium surfaces. The work by Bastasz demonstrated that the Li-dominated surfaces only exist over a few nanometers from the surface.³⁵ Fig. 6 shows deuterium irradiation of liquid and solid Sn-Li with energies between 100–1000 eV. Recall in the case of pure lithium vs deuterated Li surfaces a 1:1 retention of deuterium to lithium atoms at the surface results in the sputter yield of lithium being reduced by about 40%–50%.²⁰ The results for Sn-Li are quite different. These indicate indirectly that D uptake is negligible for tin-lithium in the solid phase. The uptake of D atoms as a function of temperature for these lithium-based alloys was found difficult to measure and has

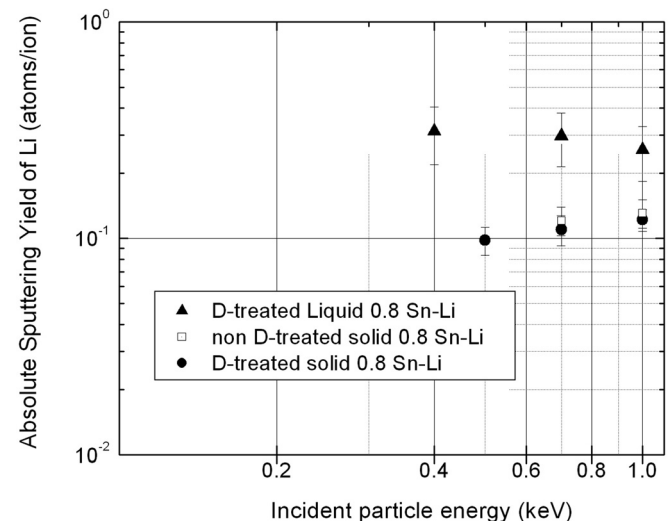


FIG. 6. Lithium sputtering from D-treated and non D-treated tin-lithium in liquid and solid phases from helium bombardment at low energies and oblique incidence.

motivated further investigation. In particular, an outstanding question remains of whether Sn-Li is truly a low-recycling (e.g., high D uptake) plasma-facing surface or not. Further work along these lines is currently underway in our laboratory. This eutectic alloy has attracted attention due to its apparent wider operational temperature window, where the non-linear temperature-dependent erosion enhancement has a threshold of a factor of 1.5–2.0 higher temperature.

C. Lithium coatings on metals

The use of liquid lithium proved promising as a low-recycling plasma-facing surface (PFS) given the results by Baldwin and Doerner for lithium's high affinity for hydrogen. However, a number of experiments conducted by Allain and Whyte *et al.*^{37,38} observed enhanced emission of lithium into the core plasma due to MHD forces induced in the conducting liquid metal. This macroscopic removal of a melted lithium layer was measured in a Li-DiMES shot during a locked-mode MHD event on DIII-D.³⁸ A temporal picture of the brightness from a visible camera tuned to neutral lithium is shown in Fig. 7. Figures 7(a)–7(c) show the temporal dependence of the Li outflux, axial current density, and incident heat flux on the DiMES lithium sample, respectively. The lithium sample crosses phase from solid to liquid between 5.089 and 5.1025 s. The lithium surface quickly

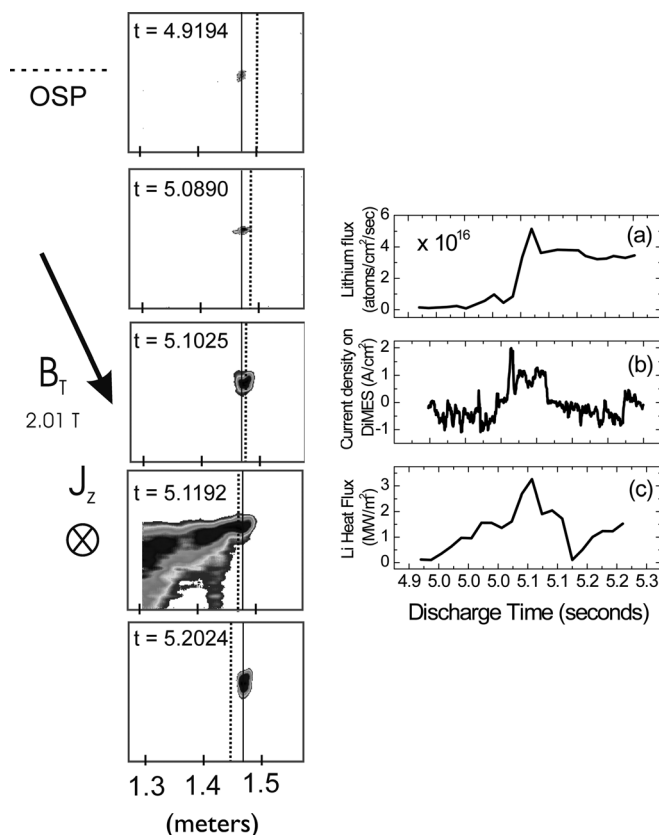


FIG. 7. Temporal picture of R+2 camera images showing removal of melted lithium during a locked mode event in DIII-D. The x-axis is in units of meters. (a) Time dependence of Li outflux measured from Li I light intensity; (b) time dependence of vertical current density onto the sample measured by floor Langmuir probes; and (c) heat flux onto lithium DiMES sample.

rises in temperature as the sample is exposed to 1.5–3.5 MW/m² heat flux over 100 ms with a maximum surface temperature near 200 °C as the heat flux peaks near 5.107 s. The cause of the large heat flux is the presence of a locked-mode MHD event, where approximately half of the core plasma stored energy is lost to the divertor in ~50 ms. However, the plasma recovers from the locked-mode and does not disrupt. The camera shows macroscopic removal of a melted lithium layer as a 2 kA/m² thermoelectric current runs through the sample during the 16 ms locked mode at approximately 5.111 s. This leads to a $j \times B$ force, which removes about 1 μm layer of lithium into the core plasma. Macroscopic erosion could lead to cases where some of this material could reach the core plasma as evidenced in Li-DiMES experiments (see Ref. 38).

These results motivated studies that would test instead of bulk liquid Li surfaces the use of thin lithium film coatings that would be subsequently melted in the hope to provide a more “adherent” lithium surface. Systematic studies elucidated how thin-film lithium coatings could be utilized to introduce controlled amounts of lithium and still provide a liquid Li surface once melted. In this section, we present experiments conducted by our group focused on studies of lithium coatings on various substrate materials to systematically understand their behavior against irradiation, temperature, and ambient impurity chemistry.

One of the first results obtained was the use of thin-film coatings on refractory metals, namely, tungsten and molybdenum. These coatings were compared to deposition of lithium on polycrystalline ATJ graphite samples with a mean roughness between 50–100 nm rms (root mean squared). Both the tungsten and molybdenum substrates are polycrystalline, 1-cm diameter with 1–2 mm thickness, and polished samples to a 10–20 nm rms roughness surface. Fig. 8 shows the results for thin lithium film coatings on ATJ graphite, Mo and W characterized with a combination of low-energy ion scattering spectroscopy (LEISS) and direct recoil spectroscopy (DRS). Only the DRS technique generates recoils from the surface. Both LEISS and DRS measure surface concentration at the top 1–2 ML. The data indicate that lithium coatings deposited on ATJ graphite leads to a “mixed” material surface (not 100% Li) indicative of lithium intercalation in graphite consistent with the literature on Li-C compounds.¹¹ Section II D will cover the lithium-carbon system in more detail.

The case for both Mo and W is consistent with 100% coverage of lithium coatings on these substrates (i.e., no intercalation effects). To test the surface properties of these films against high-intensity low-energy irradiation, a 1-keV He⁺ beam is used to irradiate a spot on a thin lithium film coating on Mo at room temperature. Atomic He is used here to avoid any chemical effects of D with Li. Room temperature is used to avoid any temperature-enhanced erosion mechanisms. Fig. 8(a) shows a photo illustrating two spots. Spot #1 consists of a region irradiated by the He⁺ beam. Spot #2 is a region characterized by LEISS that remains unirradiated. The LEISS data indicate that for Spot #1 the surface is predominantly Mo, indicating a sputtered region. LEISS was then used on that same spot but this time the

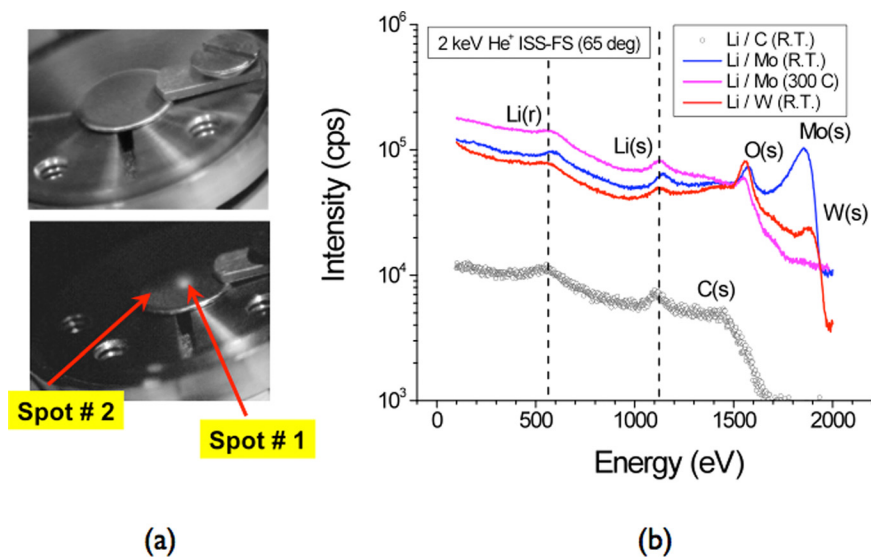


FIG. 8. (a) Photos show a molybdenum target with a deposited thin-film lithium coating (top panel) and subsequent erosion of a small spot with a He ion beam (spot #1) and nearby analysis of an unirradiated region in spot #2 (bottom panel). (b) Low-energy ion scattering spectroscopy and direct recoil spectroscopy for thin-film lithium coatings on various substrates: ATJ graphite, W and Mo. In the case of lithium films on Mo the LEISS data indicates at temperatures above 300 °C the lithium recovers the irradiated (spot #1) surface almost completely.

temperature of the Mo substrate was gradually increased to about 300 °C. The LEISS clearly shows the recovery of the pure lithium surface layer likely by surface diffusion. This result is encouraging given that if a substantial amount of lithium thin-film coatings is *sputtered atomistically* the surface can be recovered in a fusion reactor by simply raising the temperature to a moderate level near 300 °C. The work on thin-film lithium coatings was critical in elucidating their behavior under ion irradiation. One interesting aspect of this work and consistent with pure lithium work mentioned earlier along with lithium-based alloys is that for all these cases the presence of oxygen was ubiquitous. This fact motivated several compelling questions. Since previous lithium studies primarily dealt with liquid lithium with great attempts to keep the lithium surface free of any surface contaminants, how relevant is the LiD bond to lithium aided deuterium retention within a tokamak? With lithium's strong affinity to oxygen, to what degree does oxygen contribute in pumping deuterium and particle control? How would one pump deuterium if lithium coatings on graphite would diffuse and mix thus no longer able to be considered a "pure" lithium surface? These questions are studied in detail in Sec. II D.

D. Lithium coatings on ATJ graphite

As mentioned earlier, lithiated graphite surfaces were initially used in TFTR for control of fusion plasma performance. Inadvertently, significant effects were observed with TFTR plasmas and in particular on hydrogen recycling.⁸ At first, in the late 1990s when lithium-based experiments were conducted in TFTR very little was known about D-irradiated lithium coatings on graphite. Sugai *et al.* conducted a series of experiments that elucidated the role of intercalation on lithium concentrations on graphitic-based surfaces.^{9,10} These studies also demonstrated that the surface chemistry would play an important role in determining the ability for lithium coatings on graphite to pump hydrogen. However, these studies did not include much work on deuterium irradiation on lithiated graphite until the work of Allain *et al.*³⁹

Due to the initial laboratory work performed with liquid lithium based systems, deuterium was initially suspected to bind with lithium in a graphite matrix in the same manner it does in a pure liquid lithium resulting in the formation of LiD. X-ray photoelectron spectroscopy (XPS) measurements performed by Taylor *et al.* examined graphite following lithium deposition and subsequent deuterium irradiation.⁴⁰ The influence of deuterium interactions are observed indirectly in the O 1s and C 1s photoelectron energy ranges. The primary finding in this study was that deuterium interactions could be observed in the O 1s and C 1s energy regions, but only in the presence of lithium. Further studies by Taylor *et al.* show that the peaks in the O 1s and C 1s energy region grow proportional to the deuterium fluence and then become saturated at high deuterium fluences.⁴¹

The control experiments were compared to NSTX tiles that were removed from the vessel following the 2008 campaign.⁴² The tiles passivated upon air exposure and required cleaning to unbury the lithium-deuterium chemical archaeology. Remarkably, despite the boronization, lithium deposition, helium glow discharge, other wall-modifying processes, and air exposure during transit, the spectra obtained from all post-cleaned NSTX tiles aligned remarkably well (within ± 0.5 eV) with those from the controlled laboratory experiments.⁴² These results show that offline laboratory experiments establish a viable connection to understanding tokamak plasma-surface interactions. Maingi *et al.* compiled a very interesting study from NSTX that showed a direct correlation of gradual performance improvements and the deposited lithium thickness.⁴³ The intriguing part of this study is that improvements were observed continuously as deposited lithium "thickness" far exceeded the ~ 10 nm penetration depth of deuterium ions.

Besides influencing global plasma parameters, lithium "thickness" also has local effects. Taylor and Allain *et al.* found a particular NSTX tile where one radial end, that had high lithium coverage as measured using ion beam analysis, produced spectra characteristic of deuterium retention.⁴² The opposing radial end of the tile had much lower lithium coverage and lacked the deuterium-related chemistry. In order to investigate the lithium "thickness" dependence, we deposited

various lithium doses onto ATJ graphite and then bombarded with the same nominal fluence ($\sim 9 \times 10^{16} \text{ cm}^{-2}$). A high level of graphite surface morphology and rapid lithium-graphite intercalation results in effectively thinner thickness of lithium as if it were deposited on a flat substrate.^{11,40} In fact, this is the most probable cause of the continuous improvements in NSTX plasma performance Maingi observed even when the lithium “thickness” exceeded the penetration depth of the deuterium ions.⁴³

Fig. 9 shows the O 1s, C 1s, and Li 1s spectra for samples with 50, 100, 1000, and 2000 nm lithium, respectively, with a 6% error in nominal thickness. In the O 1s region, the primary peak begins to shift towards higher binding energies with higher lithium doses. Two peaks are clearly observed when 1000 nm lithium are deposited. The two O 1s peaks represent Li-O and Li-O-D interactions where Li-O is converted into Li-O-D upon deuterium irradiation. It is noteworthy that the sample with 2000 nm lithium has more intense Li-O peak (relative to the adjacent Li-O-D peak); this implies that when all samples are bombarded with 9×10^{16} ions/cm², the sample with 2000 nm lithium has more Li-O available than the samples with lower nominal doses. In the C 1s region, samples show significantly different chemistry at lower lithium doses than those observed in the O 1s region. The samples with 50 and 100 nm lithium begin to exhibit Li-C-D chemistry where deuterium related chemistry wasn't apparent in O 1s until 1000 nm.

These controls in combination with the NSTX controlled lithium deposition studies indicate that graphite yields this deuterium retention chemistry only after a minimum nominal lithium threshold is deposited on the surface. The spectra in Fig. 9 show insignificant changes with a lithium dose of 50 nm; at 100 nm lithium dose the O 1s peak shifts towards the Li-O-D reference line, and Li-C-D chemistry is observed

in the C 1s region. When a lithium dose of 1000 nm has been deposited, Li-O-D and Li-C-D chemistry are readily apparent. The O 1s and C 1s deuterium-related chemistry is always observed with 1000 nm nominal lithium dose, but not always with 100 nm lithium. These experiments in addition those in Ref. 41 indicate that the nominal threshold for observing lithium-enhanced deuterium retention exists on the range between 100 and 500 nm, and is highly dependent on the graphite surface morphology. Furthermore the correlation of the Li-O-D functionality with D irradiation also was corroborated with separate experiments that showed the role of D retention occurs dynamically during irradiation of lithiated graphite. This was work conducted by Nieto and Allain who studied the intricate mass emission during D irradiation.⁴⁴

The source of oxygen in these controlled experiments and analyzed NSTX tiles remains somewhat a mystery. In both of these cases, three sources may contribute to sourcing oxygen to the lithium. First, the lithium source may contain residual amounts of oxygen from transferring the lithium into the evaporator. In order to reduce this, transfer is performed in a flowing Ar atmosphere. The most recent lithium evaporators used in NSTX use Ar pressure to flow liquid lithium into the evaporators. Secondly, virgin ATJ graphite is found to have $\sim 5\%$ surface concentration of oxygen.⁴⁵ Finally, the ambient vacuum can contribute as an oxygen source as lithium reduces residual oxygen. In laboratory experiments, the base pressure and partial pressure of water is $< 10^{-9}$ torr, with the oxygen partial pressures typically an order of magnitude lower. In NSTX the base pressure is $\sim 10^{-8}$, and the partial pressure water flux is estimated to be $\sim 5 \times 10^{-7}$, which is in the same range as the flux of lithium.⁴⁶ This quantity of residual water is likely to contribute significantly as a source of oxygen. Because the chambers used in these laboratory experiments achieve better

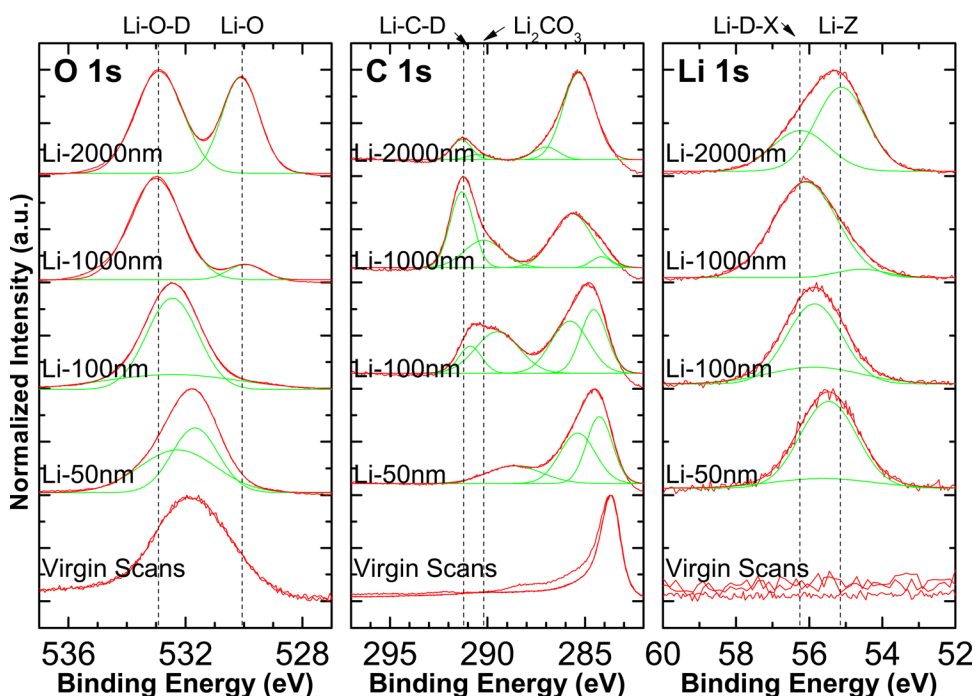


FIG. 9. O 1s, C 1s, and Li 1s spectra for samples with 50, 100, 1000, and 2000 nm lithium, respectively, with a 6% error in nominal thickness. Although lithium is apparent in the Li 1s spectrum for low doses (e.g., 50 nm), deuterium related chemistry is not observable until the lithium dose is 100–1000 nm.

pressures, impurities are easily controlled and to resemble conditions in NSTX providing an essential link in experiments.

E. Computational studies of lithium-based PMI surfaces

To elucidate on the complex behavior of liquid lithium and lithium-based coatings a number of computational simulation efforts were conducted to decipher the mechanisms responsible for deuterium retention and recycling observed in fusion edge plasmas. Controlled beam experiments presented in the earlier sections suggested the importance of surface chemistry in determining the probability for deuterium retention. However, very little effort was placed on systematic and self-consistent modeling of the Li-C-O-D system. This was primarily due to the inherent complexity in modeling such a system. In particular irradiation at low energies from D ions on a Li-C-O surface. Krstic and Allain collaborated in a series of studies that connected the *in-situ* lab experiments and advanced atomistic simulations to decipher the mechanism responsible for retention of D in Li-C-O.⁴⁷ Additional work by Krstic and Allouche elucidated on the role of lithium in retention of D in single layers of graphite.⁴⁸ Computational work corroborated the observed experimental results from XPS results summarized in Sec. II D. In particular, the simulations elucidated the role oxygen plays on retention of deuterium as opposed to lithium atoms binding as LiD. As discussed from Fig. 9, the XPS spectra of O 1s, C 1s, and Li 1s were shown. The spectra for photoelectrons collected representing the presence of oxygen were particularly important given they showed the most notable changes as a function of D irradiation dose (see Ref. 40). However, the origin of this correlation was not possible with the XPS data alone since these correspond to core-level photoelectron behavior, which make it difficult to correlate to hydrogen bonding. The atomistic quantum-mechanical simulations of Krstic *et al.*^{45,47,48} clarified this correlation showing that in fact it was the presence of *substantial* amount of oxygen on the surface (e.g., first few ML) that was necessary to induced *enhanced retention of hydrogen* in this region. Further experimental investigation by *in-situ* experiments by Taylor *et al.* found that after deposition of lithium coatings on ATJ graphite and subsequent irradiation with energetic D ions, the concentration of oxygen increases from 10% to anywhere from 20%-45% at the surface. This dramatic increase in oxygen content is currently the topic of several papers to be published soon.⁴⁹ The main result is that the simulations pointed to oxygen as the primary agent for binding of hydrogen and the presence of lithium as responsible for the increase in oxygen content *during D irradiation*. Control experiments (e.g., without lithium and with/without D irradiation) corroborated this hypothesis. Lithium, therefore, behaves as a physical catalyst that brings sufficient oxygen to the surface during D irradiation and therefore providing for a plasma-facing surface that readily pumps hydrogen by the presence of oxygen atoms. This fact explains clearly why in NSTX deposited lithium coatings were able to provide noticeable effects on plasma behavior (e.g., density control, etc...), despite the

presence of oxygen on lithium-graphite mixed surface layers.

III. CONCLUSIONS

Lithium-based surface as a candidate plasma-facing material has gained deserved attention in the last decade. Much of this attention has focused on its use as a liquid-metal PFC. However, notable advantages have also resulted from the use of lithium in various applications including: thin-film coatings on metallic substrates, lithium-graphite surfaces, lithium-based alloys, among others. There are two main challenges to the use of lithium-based surfaces as viable plasma-facing component material. One is the narrow operating temperature window for this material. At temperatures just above the melting point of lithium (e.g., 180 °C), non-linear erosion ensues and sputtering increases toward unity. The eroded lithium atoms sputter mostly as ions and the remaining neutrals quickly ionized due to lithium's low ionization potential. This fact leads to effective screening of eroded lithium material from the core plasma at all temperatures. For liquid lithium, therefore, *macroscopic* emission of material due to off-normal events such as ELMs or similar events can be problematic and thus the second challenge using lithium. However, effective application of flowing liquid Li experiments as in the case of T11-M have addressed these concerns. Lithium coatings have also shown promise and in particular as they are applied to refractory substrates such as Mo or W and also graphite. Lithium coatings have been used primarily to control hydrogen recycling and its use on various substrates has led to variable results both on retention and particle density control. Some with higher hydrogen retention (e.g., 10%–20% than non-lithiated case) based on global gas pressure measurements.

The particle density control provided by lithium coatings on graphite has enabled machines such as NSTX to reach low-recycling regimes with enhanced plasma performance (e.g., plasma confinement time, stored power, etc...). Further work consists of studying the dynamic surface effects of D irradiation on lithium-based systems such as ion-induced erosion, reflection and recycling.

¹M. G. Bell, H. W. Kugel, R. Kaita, L. E. Zakharov, H. Schneider, B. P. LeBlanc, D. Mansfield, R. E. Bell, R. Maingi, S. Ding, S. M. Kaye, S. F. Paul, S. P. Gerhardt, J. M. Canik, J. C. Hosea, and G. Taylor, *Plasma Phys. Controlled Fusion* **51**(12), 124054 (2009).

²S. Mirnov, V. Lazarev, and S. Sotnikov, *Fusion Eng. Des.* **65**(3), 455–465 (2003).

³J. Sánchez, F. L. Tabarés, D. Tafalla, J. A. Ferreira, I. García-Cortés, C. Hidalgo, F. Medina, M. A. Ochando, M. A. Pedrosa, and TJ-II Team, *J. Nucl. Mater.* **390–391**, 852–857 (2009).

⁴A. Tuccillo, A. Alekseyev, B. Angelini, S. V. Annibaldi, M. Apicella, G. Apruzzese, J. Berrino, E. Barbato, A. Bertocchi, and A. Biancalani, *Nucl. Fusion* **49**, 104013 (2009).

⁵G. Xu, B. Wan, J. Li, X. Gong, J. Hu, J. Shan, H. Li, D. Mansfield, D. Humphreys, and V. Naulin, *Nucl. Fusion* **51**, 072001 (2011).

⁶S. Munaretto, S. Dal Bello, P. Innocente, M. Agostini, F. Auriemma, S. Barison, A. Canton, L. Carraro, G. De Masi, S. Fiameni, P. Scarin, and D. Terranova, *Nucl. Fusion* **52**, 023012 (2012).

⁷S. Erents, G. McCracken, and P. Goldsmith, *J. Phys. D: Appl. Phys.* **4**, 672 (1971).

⁸D. Mansfield, D. Johnson, B. Grek, H. Kugel, M. Bell, R. Bell, R. Budny, C. Bush, E. Fredrickson, and K. Hill, *Nucl. Fusion* **41**, 1823 (2001).

- ⁹H. Sugai, H. Toyoda, K. Nakamura, K. Furuta, M. Ohori, K. Toi, S. Hirokura, and K. Sato, *J. Nucl. Mater.* **220**, 254–258 (1995).
- ¹⁰H. Toyoda, M. Watanabe, and H. Sugai, *J. Nucl. Mater.* **241**, 1031–1035 (1997).
- ¹¹N. Itou, H. Toyoda, K. Morita, and H. Sugai, *J. Nucl. Mater.* **290**, 281–285 (2001).
- ¹²M. Abdou, *Fusion Eng. Des.* **54**(2), 181–247 (2001).
- ¹³R. F. Mattas, J. P. Allain, R. Bastasz, J. N. Brooks, T. Evans, A. Hassanein, S. Luckhardt, K. McCarthy, P. Mioduszewski, and R. Maingi, *Fusion Eng. Des.* **49**, 127–134 (2000).
- ¹⁴J. Brooks, J. P. Allain, R. Bastasz, R. Doerner, T. Evans, A. Hassanein, R. Kaita, S. Luckhardt, R. Maingi, and R. Majeski, *Fusion Sci. Technol.* **47**(3), 669–677 (2005).
- ¹⁵M. Baldwin, R. Doerner, R. Causey, S. Luckhardt, and R. Conn, *J. Nucl. Mater.* **306**(1), 15–20 (2002).
- ¹⁶M. Baldwin, R. Doerner, S. Luckhardt, and R. Conn, *Nucl. Fusion* **42**, 1318 (2002).
- ¹⁷M. Baldwin, R. Doerner, S. Luckhardt, R. Seraydarian, D. Whyte, and R. Conn, *Fusion Eng. Des.* **61**, 231–236 (2002).
- ¹⁸R. Doerner, M. Baldwin, S. Krashenninnikov, and D. Whyte, *J. Nucl. Mater.* **313**, 383–387 (2003).
- ¹⁹R. Bastasz and J. Whaley, *Fusion Eng. Des.* **72**(1), 111–119 (2004).
- ²⁰J. P. Allain and D. Ruzic, *Nucl. Fusion* **42**, 202 (2002).
- ²¹R. Majeski, M. Boaz, D. Hoffman, B. Jones, R. Kaita, H. W. Kugel, T. Munsat, J. Spaleta, V. A. Soukhanovskii, and J. Timberlake, *J. Nucl. Mater.* **313**, 625–629 (2003).
- ²²R. Majeski, S. Jardin, R. Kaita, T. Gray, P. Marfuta, J. Spaleta, J. Timberlake, L. E. Zakharov, G. Antar, and R. Doerner, *Nucl. Fusion* **45**, 519 (2005).
- ²³H. Kugel, V. Soukhanovskii, M. Bell, W. Blanchard, D. Gates, B. Leblanc, R. Maingi, D. Mueller, H. Na, and S. Paul, *J. Nucl. Mater.* **313**, 187–193 (2003).
- ²⁴H. W. Kugel, M. G. Bell, J. Ahn, J. P. Allain, R. E. Bell, J. A. Boedo, C. E. Bush, D. A. Gates, T. Gray, and S. M. Kaye, *Phys. Plasmas* **15**(5), 056118 (2008).
- ²⁵J. Hogan, C. Bush, and C. Skinner, *Nucl. Fusion* **37**, 705 (1997).
- ²⁶R. Doerner, M. Baldwin, R. Conn, A. Grossman, S. Luckhardt, R. Seraydarian, G. Tynan, and D. Whyte, *J. Nucl. Mater.* **290**, 166–172 (2001).
- ²⁷R. Bastasz, J. Medlin, J. Whaley, R. Beikler, and E. Taglauer, *Surf. Sci.* **571**(1–3), 31–40 (2004).
- ²⁸J. P. Allain, D. Ruzic, and M. Hendricks, *J. Nucl. Mater.* **290**, 33–37 (2001).
- ²⁹J. P. Allain, M. Coventry, and D. Ruzic, *J. Nucl. Mater.* **313**, 641–645 (2003).
- ³⁰J. P. Allain, D. Ruzic, D. Alman, and M. Coventry, *Nucl. Instrum. Methods Phys. Res. B* **239**(4), 347–355 (2005).
- ³¹J. P. Allain, D. Whyte, and J. Brooks, *Nucl. Fusion* **44**, 655 (2004).
- ³²S. Mirnov, E. Azizov, V. Evtikhin, V. Lazarev, I. Lyublinski, A. Vertkov, and D. Y. Prokhorov, *Plasma Phys. Controlled Fusion* **48**, 821 (2006).
- ³³J. P. Allain, M. Coventry, and D. Ruzic, *Phys. Rev. B* **76**(20), 205434 (2007).
- ³⁴M. Thompson, *Philos. Trans. R. Soc. London* **362**(1814), 5–28 (2004).
- ³⁵R. Bastasz and W. Eckstein, *J. Nucl. Mater.* **290**, 19–24 (2001).
- ³⁶J. N. Brooks, T. D. Rognlien, D. N. Ruzic, and J. P. Allain, *J. Nucl. Mater.* **290–293**, 185–190 (2001).
- ³⁷J. P. Allain, M. Nieto, M. Coventry, R. Stubbers, and D. Ruzic, *Fusion Eng. Des.* **72**(1), 93–110 (2004).
- ³⁸D. G. Whyte, T. E. Evans, C. P. Wong, W. P. West, R. Bastasz, J. P. Allain, and J. N. Brooks, *Fusion Eng. Des.* **72**(1), 133–147 (2004).
- ³⁹J. P. Allain, D. Rokusek, S. Harilal, M. Nieto-Perez, C. Skinner, H. Kugel, B. Heim, R. Kaita, and R. Majeski, *J. Nucl. Mater.* **390**, 942–946 (2009).
- ⁴⁰C. N. Taylor, B. Heim, and J. P. Allain, *J. Appl. Phys.* **109**(5), 053306 (2011).
- ⁴¹C. N. Taylor, J. P. Allain, B. Heim, P. S. Krstic, C. H. Skinner, and H. W. Kugel, *J. Nucl. Mater.* **415**(1), S777 (2011).
- ⁴²C. N. Taylor, K. E. Luitjohan, B. Heim, L. Kollar, J. P. Allain, C. H. Skinner, H. W. Kugel, R. Kaita, A. L. Roquemore, and R. Maingi, “Surface chemistry analysis of lithium conditioned NSTX graphite tiles correlated to plasma performance,” *Nucl. Fusion* (submitted).
- ⁴³R. Maingi, S. Kaye, C. Skinner, D. Boyle, J. Canik, M. Bell, R. Bell, T. Gray, M. Jaworski, R. Kaita, H. Kugel, B. Leblanc, D. Mansfield, T. Osborne, S. Sabbagh, and V. A. Soukhanovskii, *Phys. Rev. Lett.* **107**(14), 145004 (2011).
- ⁴⁴M. Nieto-Perez, J. P. Allain, B. Heim, and C. N. Taylor, *J. Nucl. Mater.* **415**, S133 (2011).
- ⁴⁵P. S. Krstic, J. P. Allain, C. N. Taylor, J. Dadrás, S. Maeda, K. Morokuma, J. Jakowski, A. Allouche, and C. Skinner, “Tuning fusion plasma behavior at the nanoscale on lithium-based surfaces,” *Sci. Rep.* (submitted).
- ⁴⁶C. Skinner, M. Jaworski, H. Kugel, R. Majeski, R. Kaita, V. Surla, R. Sul-lenberger, and B. Koel, 53rd Annual Meeting of the APS Division of Plasma Physics, Salt Lake City, Utah 2011.
- ⁴⁷P. S. Krstic, J. P. Allain, A. Allouche, J. Jakowski, J. Dadrás, C. N. Taylor, and Z. Yang, *Fusion Eng. Des.* (to be published).
- ⁴⁸A. Allouche and P. S. Krstic, *Carbon* **50**(2), 347–740 (2011).
- ⁴⁹C. N. Taylor, J. P. Allain, K. E. Luitjohan, P. S. Krstic, J. Dadrás, and C. H. Skinner, “The role of oxygen in retaining deuterium on lithiated graphite surfaces,” *J. Nucl. Mater.* (submitted).